


Article

The Crystal Chemistry of Voltaite-Group Minerals from Post-Volcanic and Anthropogenic Occurrences

Elena S. Zhitova ^{1,*} , Rezeda M. Sheveleva ^{1,2}, Anastasia N. Kupchinenko ¹ , Andrey A. Zolotarev ² , Igor V. Pekov ³, Anton A. Nuzhdaev ¹, Vesta O. Davydova ³ , Natalia S. Vlasenko ², Ekaterina Y. Plutakhina ¹ , Vasilii O. Yapaskurt ³, Peter E. Schweigert ¹ and Tatiana F. Semenova ²

¹ Institute of Volcanology and Seismology, Far East Branch of Russian Academy of Sciences, Piip Blvd. 9, 683006 Petropavlovsk-Kamchatsky, Russia; r.sheveleva@spbu.ru (R.M.S.); kupchasta@yandex.ru (A.N.K.); envi@kscnet.ru (A.A.N.); peu@kscnet.ru (E.Y.P.)

² Saint-Petersburg State University, University Embankment, 7/9, 199034 Saint-Petersburg, Russia; a.zolotarev@spbu.ru (A.A.Z.); n.vlasenko@spbu.ru (N.S.V.); t.semenova@spbu.ru (T.F.S.)

³ Faculty of Geology, Moscow State University, Leninskie Gory, 1, 119991 Moscow, Russia; igorpekov@geol.msu.ru (I.V.P.); davydovavo@my.msu.ru (V.O.D.)

* Correspondence: e.zhitova@spbu.ru or zhitova_es@mail.ru

Abstract: Five samples of voltaite-group minerals from post-volcanic occurrences (geothermal fields and solfatara at pyroclastic flow) and from pseudofumaroles born by coal fires are characterized by single-crystal X-ray diffraction, scanning electron microscopy and electron microprobe analysis. The studied minerals include ammoniomagnesiovoltaite, ammoniovoltaite, voltaite and magnesiovoltaite. The quadrilateral of chemical compositions is determined by monovalent cations such as $(\text{NH}_4)^+$ and K^+ and divalent cations such as Fe^{2+} and Mg^{2+} . Minor Al can occur in the Fe^{3+} site. Minor amounts of P, V can occur in the S site. Ammonium members are described from geothermal fields, expanding the mineral potential of this type of geological environment. All minerals are cubic, space group $Fd-3c$, $a = 27.18\text{--}27.29$ Å, $V = 20079\text{--}20331$ Å³, $Z = 16$. No clear evidence of symmetry lowering (suggested for synthetic voltaites) is observed despite the chemical variation in the studied samples. Ammonium species tend to have a larger a lattice parameter than potassium ones due to longer $\langle A\text{--O} \rangle$ distances ($A = \text{N}$ or K). The systematically shorter $\langle \text{Me}^{2+}\text{--}\phi \rangle_{\text{obs}}$ ($\text{Me}^{2+} = \text{Fe}, \text{Mg}$; $\phi = \text{O}, \text{H}_2\text{O}$) in comparison to $\langle \text{Me}^{2+}\text{--}\phi \rangle_{\text{calc}}$ bond lengths can be explained as a consequence of mean bond length variation due to significant bond length distortion in $\text{Me}^{2+}\phi_6$ octahedra $\text{Me}2\text{--O}2\text{--}2.039\text{--}2.055$ Å; $\text{Me}2\text{--O}4\text{--}2.085\text{--}2.115$ Å; and $\text{Me}2\text{--O}w5\text{--}2.046\text{--}2.061$ Å, with bond length distortion estimated as from 0.008 to 0.014 for different samples.

Keywords: voltaite; magnesiovoltaite; ammoniovoltaite; ammoniomagnesiovoltaite; volcano; fumarole; coal fire; crystal structure; pseudofumarole; Kamchatka



Citation: Zhitova, E.S.; Sheveleva, R.M.; Kupchinenko, A.N.; Zolotarev, A.A.; Pekov, I.V.; Nuzhdaev, A.A.; Davydova, V.O.; Vlasenko, N.S.; Plutakhina, E.Y.; Yapaskurt, V.O.; et al. The Crystal Chemistry of Voltaite-Group Minerals from Post-Volcanic and Anthropogenic Occurrences. *Symmetry* **2023**, *15*, 2126. <https://doi.org/10.3390/sym15122126>

Academic Editor: György Keglevich

Received: 30 October 2023

Revised: 19 November 2023

Accepted: 22 November 2023

Published: 29 November 2023



Copyright: © 2023 by the authors. Licensee MDPI, Basel, Switzerland. This article is an open access article distributed under the terms and conditions of the Creative Commons Attribution (CC BY) license (<https://creativecommons.org/licenses/by/4.0/>).

1. Introduction

The voltaite group includes hydrous sulfate minerals with the general formula $A_2\text{Me}_2\text{M}_1\text{Al}(\text{SO}_4)_{12}(\text{H}_2\text{O})_{18}$, where species-defining cations are $A = (\text{NH}_4)^+$, K ; $\text{Me}2 = \text{Fe}^{2+}$, Mg , Zn ; $\text{M}1 = \text{Fe}^{3+}$ or Fe^{3+} combined with Mg [1–6]. Synthetic voltaite-like sulfates were reported with $A = (\text{NH}_4)^+$, K , Tl , Rb and $\text{Me}2 = \text{Fe}^{2+}$, Mg , Zn , Cd , Co and Mn [7–14].

The crystal structure of voltaite consists of krönkite-like chains in which $\text{Me}^{2+}\phi_6$ ($\phi = \text{O}, \text{H}_2\text{O}$) octahedra are corner-shared to sulfate tetrahedra that, in turn, are corner-shared with $\text{M}1\text{O}_6$ ($\text{M}1 = \text{Fe}^{3+}$) octahedra. The three-dimensional arrangement of such chains produces the framework, with two types of cavities occupied by A -site cations and $\text{Al}(\text{H}_2\text{O})_6$ octahedra [12,15] (Figure 1). Most of the voltaite-group minerals are cubic, $Fd-3c$, with the exception of pertlikite which is tetragonal, $I4_1/acd$, as the result of symmetry lowering due to Fe-Mg ordering in one crystallographic site [3,4,12,16–18]. For synthetic samples [12], cubic and tetragonal modifications were observed forming even sectorial

crystals. The estimation of information-based structural complexity using crystal structure data [19] shows that the voltaite-group minerals are very complex with structural complexity per atom (I_G) and per unit cell ($I_{G,\text{total}}$) being 4.160 bit/atom and 3177.944 bit/cell, as calculated for one published voltaite model [17]. The high complexity of the voltaite framework is the combination of topological information (~30%); interstitial structure (~20%) and hydrogen bonding network (>50%) with some authors [19] suggesting even higher complexity for the ammonium representatives of the voltaite group. In that work [19], the authors note the high complexity of the general voltaite framework and suggest that this is responsible for the high structural complexity.

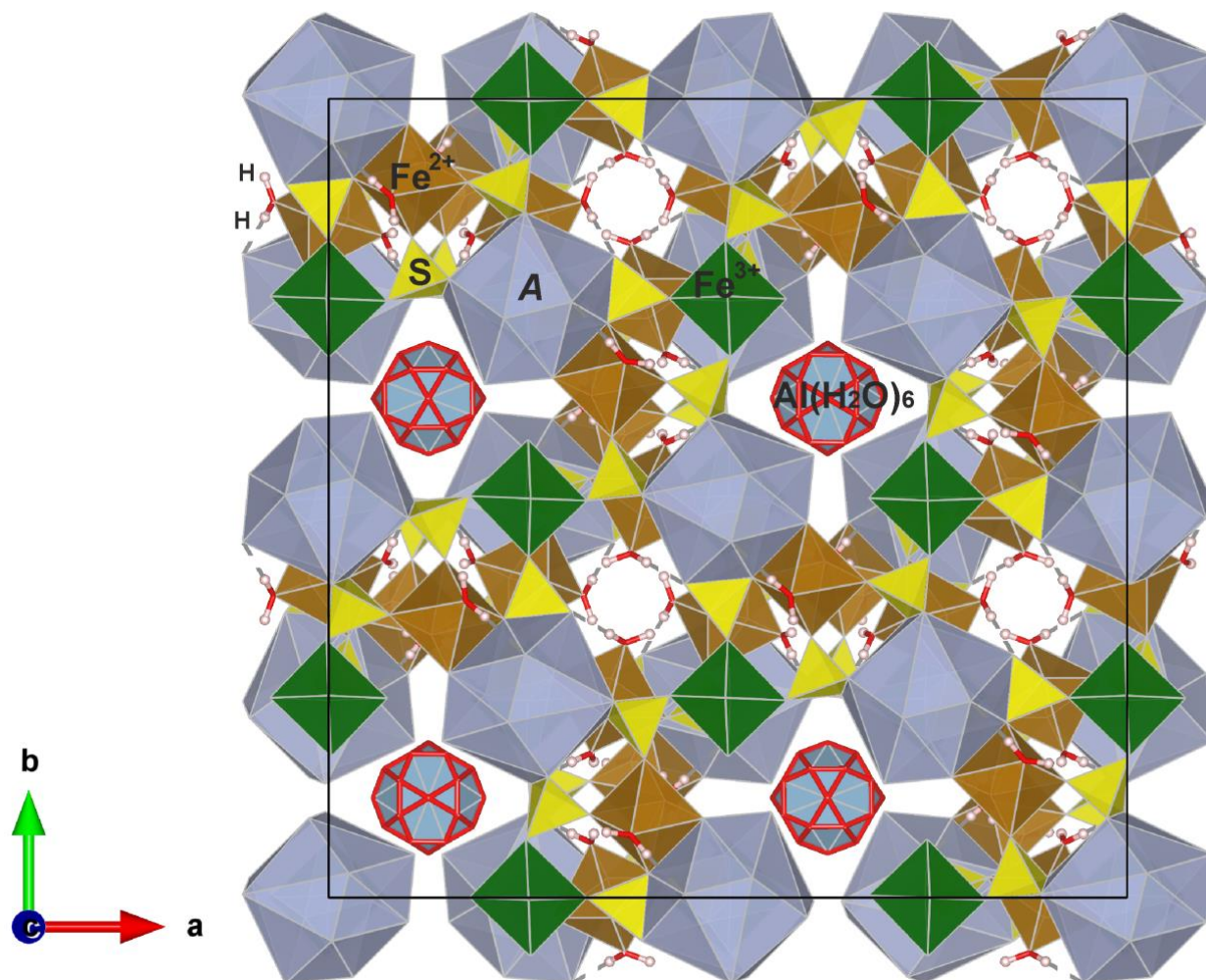


Figure 1. The crystal structure of cubic voltaite-group minerals. The polyhedra notification is shown and the unit-cell is outlined (by black line), the crystallographic axes are shown.

The formation of voltaite-group minerals tends to occur under acid leaching conditions at temperatures typically not higher than 100 °C. In nature, these are mainly conditions like low-temperature volcanic fumaroles (solfatares), gas-steam jets of hydrothermal activity at geothermal fields and the oxidation zone of sulfide ores, commonly in arid regions. The coal fires with exhalations deposited around pseudofumaroles have “near-natural”, or anthropogenic (technogenic) origin, while voltaite formation in acid mine drainage (AMD) settings is definitely the result of an anthropogenic process [12].

Recently, Tl-bearing voltaite was described from the Apuan Alps (Tuscany, Italy) [17], expanding the chemical composition of natural species. This is important from an environmental point of view since Tl-bearing voltaites could be the long-term source and sink of Tl in surface environments [20]. At the same time, the findings of ammonium members of

the voltaite group reflect rather unusual geochemical features of a mineral formation system. Recently ammoniovoltaite, $(\text{NH}_4)_2\text{Fe}^{2+}_5\text{Fe}^{3+}_3\text{Al}(\text{SO}_4)_{12}(\text{H}_2\text{O})_{18}$, has been described as a new mineral from the Severo-Kambalny geothermal field (Kamchatka, Russia) [6] that is deposited around steam-gas jets and has not been described from other localities yet. A similar situation is observed for ammoniomagnesiovoltaite, first described from anthropogenic pseudofumaroles at the burning dumps of coal mines in 2009 [4] and that has a couple of confirmed findings worldwide. This somewhat contrasts with the findings of potassium voltaites, which are tens of times more numerous. Interestingly, “ordinary” potassium voltaite, i.e., potassic voltaite, has been described from the Geysers geothermal system, California, USA [21] where many ammonium minerals were also reported.

Ammonium-dominant group species are still described very scarcely in terms of their crystal structure (one structure refinement using single-crystal XRD data [6]) and abundance. The present work is intended to provide the chemical composition and crystal structure data for five samples of voltaite-group minerals and an analysis of their geometrical parameters. Separately, we note that voltaite-group minerals are rather common for post-volcanic environments, however they are rarely described in detail from this type of occurrence.

2. Materials and Methods

2.1. Materials

This paper presents a study of voltaite-group minerals from the objects of two different genetic types: (a) natural conditions related to acid leaching, with water solutions or fumarolic gases in the area of active volcanism and (b) natural or anthropogenic coal fire.

Regarding voltaite-group minerals from post-volcanic occurrences, the four samples presented here occur from four volcanos (all located at Kamchatka, Far East Russia): Koshelev, Bolshoi Semiachik, Mutnovsky and Shiveluch. The temperature of mineral formation in all cases is estimated as not higher than 100 °C. The minerals formed around steam-gas jets and at the surface of geothermal fields (Figure 2).

The samples from geothermal fields were well-shaped isometric crystals of voltaite-group minerals up to 0.13 mm or clusters of smaller isometric crystals of black, dark-green, oil-green or grey colour occurring in intimate association with halotrichite and/or alunogen (Figure 2c,d). The samples from geothermal fields are denoted as the following (abbreviation—name of thermal field): VK—Verkhne-Koshelev (Koshelev volcano); Dch—Dachnoe (Muntnovsky volcano); SCC—Severny (=North) Crater of Centralny (=Central) Semiachik (Bolshoi Semiachik volcanic complex). Some chemical and structural features of halotrichite, alunogen, alunite-group and alum-group members and other minerals found in association with voltaite-group sulfates from these localities were discussed recently [22–24].

At Shiveluch volcano, voltaite-group minerals were formed in low-temperature sulfate fumaroles (solfatares) at pyroclastic deposits that appeared after a strong volcanic eruption in April 2023 (Figure 2b). In the sample Shiv-8030, magnesiovoltaite occurs as well-shaped grey crystals up to 0.1 mm across, formed by {110}, {100} and {111} faces, and with clusters associated with pickeringite, godovikovite, alunogen, tamarugite, Fe-bearing kieserite, mascagnite, adranosite, and boussingaultite.

Anthropogenic voltaite studied in this work is represented by the sample collected in 1988 at the burning terricon of the Yuriy Gagarin coal mine located in Nikitovka, Donetsk Oblast of the Ukrainian SSR. Voltaite forms open-work aggregates of green-black cuboctahedral crystals up to 0.05 mm closely associated with colourless alunogen in sublimates of a pseudofumarole.

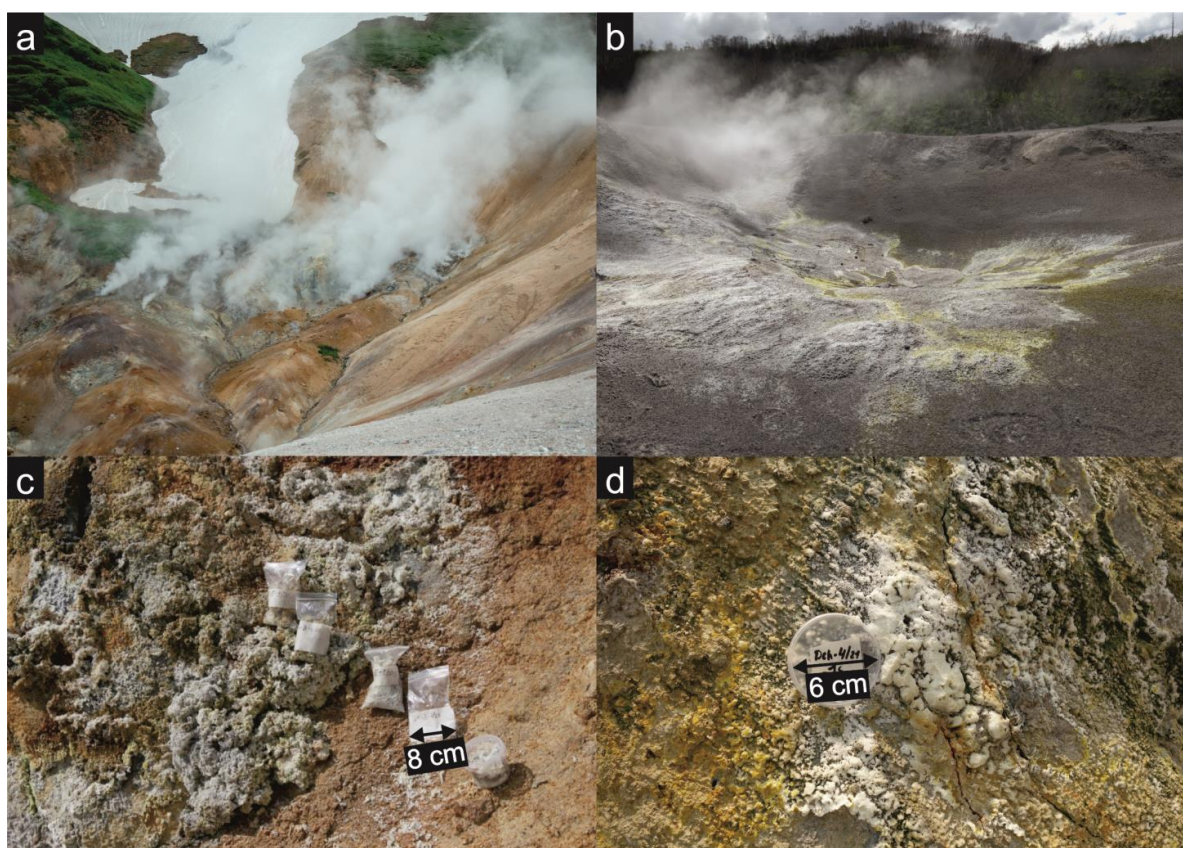


Figure 2. The locations of mineral sampling: (a) geothermal field Severny Crater of Centralny Semiachik; (b) solfatares at pyroclastic deposits of Shiveluch; (c) efflorescent samples from Severny Crater of Centralny Semiachik; and (d) efflorescent samples from Dachnoe geothermal field, Mutnovsky volcano (the box has a number).

2.2. Methods

2.2.1. Scanning Electron Microscopy (SEM) and Electron Microprobe Analysis (EMPA)

Voltaite-group minerals were prepared for analysis in two ways: (i) deposited on carbon tape, then carbon coated and (ii) immersed into epoxy resin that was polished after hardening and finally carbon coated. The samples were studied using SEM and EMPA (energy-dispersive spectroscopy (EDS) mode). EDS, but not wavelengths-dispersive spectroscopy (WDS), was used due to the possibility of (1) performing analyses with low beam current which is necessary due to the instability of the highly hydrous minerals under electron beam and (2) in situ control of the sample condition during the spectrum acquisition, as well as the analysis of small-sized grains of distinct minerals found in intimate association [25,26].

The chemical composition of voltaite-group minerals was analysed using electron microscopes at three locations: (i) the “Geomodel” Resource Centre of the Scientific Park of St. Petersburg State University, which has a scanning electron microscope Hitachi S-3400N (Hitachi Ltd., Tokyo, Japan) equipped with an energy-dispersive spectrometer Oxford X-Max 20 (Oxford Instruments Ltd., Abingdon, UK), operating at an accelerating voltage of 20 kV and a probe current of 0.5 nA with various electron beam diameters of minimum 5 μm due to possible dehydration under the electron beam; (ii) the Laboratory of Volcanogenic Ore Formation of the Institute of Volcanology and Seismology FEB RAS, which has a scanning electron microscope Tescan Vega 3 LMH (Tescan Ltd., Prague, Czech Republic) equipped with an energy-dispersive spectrometer Oxford X-Max 80 mm² (Oxford Instruments Ltd., UK), operating at an accelerating voltage of 20 kV, current intensity of 0.9 nA and beam size of 220 nm, with analyses carried out in areas of about 5 \times 5 μm ;

(iii) the Laboratory of Local Methods of Matter Investigation, Faculty of Geology, Moscow State University, which has a Jeol JSM-6480LV scanning electron microscope equipped with an energy-dispersive spectrometer X-Max 50, at an acceleration voltage of 20 kV, a beam current of 0.7 nA, and a 5 μm beam diameter. The scanning electron microscope Hitachi S-3400N was calibrated against a series of natural standards (MAC). For the scanning electron microscope Tescan Vega 3 LMH system, calibration was performed on Ni. The following standards were used: pure metals (Fe, Cu), corundum (Al), herzenbergite (S), sanidine (K, Na, Si), periclase (Mg). For the analysis on Jeol JSM-6480LV the following standards were used: orthoclase (K), diopside (Mg), Al_2O_3 (Al), Ti (Ti), FeS (Fe), and BaSO_4 (S). The resulting data were processed using the AZtec program package in all cases.

2.2.2. Single-Crystal X-ray Diffraction

Single-crystal X-ray diffraction analysis was carried out for voltaite-group minerals using Rigaku XtaLAB Synergy-S (Rigaku corporation, Akishima, Japan) operated with monochromated $\text{MoK}\alpha$ radiation (source: $\text{MoK}\alpha$, $\lambda = 0.71073 \text{ \AA}$) at 50 kV and 1.0 mA and equipped with a CCD HyPix-6000HE detector (Rigaku corporation, Japan). The conditions of data collection are given in Table 1. The CrysAlisPro [27] software package was used to process the data; an empirical absorption correction was calculated based on spherical harmonics implemented in the SCALES ABSPACK algorithm. The structures were solved and refined using the ShelX program package [28] incorporated into the Olex2 software shell [29].

Table 1. Crystal chemical data, data collection and refinement parameters for voltaite-group minerals.

Sample	VK4-09	Dch-9-21-5s	Ni4225	SCCIII-14-20s	Shiv-8030
Crystal Chemical Data					
Crystal system	Cubic	Cubic	Cubic	Cubic	Cubic
Space group	<i>Fd-3c</i>	<i>Fd-3c</i>	<i>Fd-3c</i>	<i>Fd-3c</i>	<i>Fd-3c</i>
<i>a</i> (\AA)	27.2933 (5)	27.2464 (3)	27.2364 (6)	27.1801 (2)	27.1921 (2)
<i>V</i> (\AA^3)	20,331.4 (11)	20,226.8 (7)	20,204.6 (13)	20,079.5 (4)	20,106.0 (3)
<i>Z</i>	16	16	16	16	16
Calculated density (g/cm^3)	2.454	2.498	2.511	2.540	2.525
Absorption coefficient (mm^{-1})	2.124	2.325	2.272	2.294	2.194
Size, mm	$0.09 \times 0.09 \times 0.09$	$0.05 \times 0.05 \times 0.05$	$0.06 \times 0.06 \times 0.06$	$0.08 \times 0.10 \times 0.12$	$0.09 \times 0.09 \times 0.09$
Colour	Green	Dark grey	Black	Black	Grey
Data collection					
Temperature (K)	293	293	293	293	293
Radiation, wavelength (\AA)			$\text{MoK}\alpha$, 0.71073		
Range of data collection, 2θ ($^\circ$)	7.314–66.79	7.326–67.596	7.33–66.948	7.344–67.38	7.34–70.92
<i>h</i> , <i>k</i> , <i>l</i> ranges	$-38 \rightarrow 29$, $-41 \rightarrow 23$, $-14 \rightarrow 37$	$-30 \rightarrow 41$, $-42 \rightarrow 34$, $-30 \rightarrow 30$	$-15 \rightarrow 37$, $-24 \rightarrow 41$, $-38 \rightarrow 29$	$-42 \rightarrow 42$, $-37 \rightarrow 41$, $-40 \rightarrow$ 41	$-27 \rightarrow 34$, $-35 \rightarrow 44$, $-43 \rightarrow 19$
Total reflection collected	8961	12,822	9942	84,994	23,593
Unique reflections	1481	1488	1477	1632	1814
(R_{int})	(0.0572)	(0.0361)	(0.0493)	(0.0672)	(0.0286)
Number of unique reflections $F > 2\sigma(F)$	1185	1204	1229	1208	1630
Data completeness (%)	99.5	99.5	99.6	99.6	99.6
Structure refinement					
Refinement method	Full-matrix least-squares on F^2				
Weighting coefficients a, b	0.0394, 474.1972	0.0386, 64.5360	0.0112, 365.3476	0.0448, 423.1603	0.0445, 48.4126
Data/restrain/parameters	1481/2/95	1488/2/95	1477/2/95	1632/2/95	1814/2/94
R_1 [$F > 2\sigma(F)$], wR_2 [$F > 2\sigma(F)$]	0.0590, 0.1237	0.0331, 0.0758	0.0521, 0.0991	0.0507, 0.1144	0.0250, 0.0727
R_1 all, wR_2 all	0.0777, 0.1324	0.0478, 0.0806	0.0665, 0.1024	0.0847, 0.1480	0.0293, 0.0743
Goodness-of-fit on F^2	1.176	1.092	1.257	1.238	1.152
Largest diff. peak and hole (\AA^{-3})	0.63/−0.93	0.45/−0.30	0.47/−0.52	0.75/−0.55	0.51/−1.13

3. Results

3.1. Crystal Structure

As an initial structure model for the refinement, the atomic coordinates were taken from 6 for ammoniovoltaite. The H atoms of the H₂Ow5 molecule coordinating Me2 site were located from the analysis of difference Fourier electron-density maps and were refined with imposed restraints of $0.9 \pm 0.02 \text{ \AA}$ [30]. H-atom positions for H₂O molecules in Al(H₂O)₆ octahedra were not refined due to disordering of H₂O molecules (even O-atoms). There is a correlation between the crystal quality (that is reflected by R_{int} , which is the measure of equivalence of symmetry-equivalent reflections) and the disagreement index R_1 (that is equivalent to obtaining a least-squares fit between the calculated electron density and that obtained from a Fourier series based on the observed structure factors) [31]. As such, the crystal structure of better crystallized crystal is refined to lower disagreement indexes. However, all disagreement indexes are rather low.

The crystal structure of the voltaite-group minerals consists of an A site occupied by monovalent cations, either N (of NH₄) or K, in different proportions (Table 2). The Me2 site accommodates mainly Fe and Mg cations in different proportions (Table 2). Selected bond distances for the voltaite-group minerals are provided in Table 3. The analyses of bond lengths show that variation in them is negligible in Fe³⁺-centered polyhedra (in the range 2.001–2.008 Å) and prominent in Me2 (Fe/Mg-centered) octahedra (2.064–2.073 Å), reflecting wide isomorphism of the divalent cation.

Table 2. Atom coordinates, equivalent isotropic displacement parameters and site occupancies for the voltaite-group minerals.

Atom	x	y	z	U_{eq}	s.o.f.	x	Y	Z	U_{eq}	s.o.f.
VK4-09						Dch-9-21-5s				
N1	1/4	1/4	1/4	0.033(3)	0.893(17)	1/4	1/4	1/4	0.044(2)	0.850(11)
K1	1/4	1/4	1/4	0.033(3)	0.107(17)	1/4	1/4	1/4	0.044(2)	0.150(11)
Fe1	1/4	1/4	0	0.0136(2)	1	1/4	1/4	0	0.0183(2)	1
Fe2	0.35294(3)	1/4	0.14706(3)	0.0151(3)	0.501(8)	0.35239(2)	1/4	0.14761(2)	0.0191(2)	0.617(4)
Mg2	0.35294(3)	1/4	0.14706(3)	0.0151(3)	0.499(8)	0.35239(2)	1/4	0.14761(2)	0.0191(2)	0.383(4)
Al*	1/8	1/8	1/8	0.0128(6)	1	1/8	1/8	1/8	0.0164(4)	1
S1	0.23786(3)	0.27576(3)	0.11789(3)	0.0135(2)	1	0.23727(2)	0.27579(2)	0.11778(2)	0.01879(12)	1
O1	0.24970(11)	0.24707(10)	0.07325(9)	0.0194(5)	1	0.24988(5)	0.24698(5)	0.07337(5)	0.0239(3)	1
O2	0.22506(12)	0.32628(10)	0.10434(11)	0.0252(6)	1	0.22530(7)	0.32639(6)	0.10411(6)	0.0315(4)	1
O3	0.19572(12)	0.25413(12)	0.14254(13)	0.0305(7)	1	0.19410(7)	0.25448(6)	0.14133(7)	0.0359(4)	1
O4	0.28047(11)	0.27504(12)	0.15080(10)	0.0243(6)	1	0.27932(6)	0.27485(7)	0.15154(5)	0.0335(4)	1
OW5	0.32848(13)	0.18105(12)	0.12829(12)	0.0283(7)	1	0.32845(7)	0.18079(6)	0.12877(7)	0.0337(4)	1
H5A	0.305(2)	0.170(2)	0.147(2)	0.07(2)	1	0.306(1)	0.171(1)	0.150(1)	0.08(1)	1
H5B	0.333(4)	0.169(4)	0.098(2)	0.14(4)	1	0.319(2)	0.182(2)	0.098(1)	0.17(3)	1
OW6	0.1036(4)	0.1795(4)	0.0890(4)	0.021(2)	0.234(2)	0.1031(2)	0.1790(2)	0.0890(2)	0.0272(13)	0.247(2)
OW7	0.1460(5)	0.1802(4)	0.0892(5)	0.020(3)	0.215(2)	0.1467(2)	0.1797(2)	0.0886(2)	0.0260(13)	0.234(2)
OW8	1/8	0.1938(11)	1/8	0.007(5)	0.102(3)	1/8	0.1954(12)	1/8	0.002(7)	0.039(3)
Ni4225						SCCIII-14-20s				
N1	1/4	1/4	1/4	0.0309(10)	0.365(14)	1/4	1/4	1/4	0.0368(8)	0.088(16)
K1	1/4	1/4	1/4	0.0309(10)	0.635(14)	1/4	1/4	1/4	0.0368(8)	0.912(16)
Fe1	1/4	1/4	0	0.0129(2)	1	1/4	1/4	0	0.0196(3)	1
Fe2	0.35271(2)	1/4	0.14729(2)	0.0131(3)	0.531(7)	0.35285(3)	1/4	0.14715(3)	0.0206(3)	0.508(8)
Mg2	0.35271(2)	1/4	0.14729(2)	0.0131(3)	0.469(7)	0.35285(3)	1/4	0.14715(3)	0.0206(3)	0.492(8)
Al*	1/8	1/8	1/8	0.0110(6)	1	1/8	1/8	1/8	0.0184(6)	1
S1	0.23721(3)	0.27563(3)	0.11809(3)	0.0140(2)	1	0.23771(3)	0.27550(3)	0.11851(3)	0.0196(2)	1
O1	0.24991(10)	0.24658(10)	0.07366(8)	0.0210(5)	1	0.24965(10)	0.24674(10)	0.07374(9)	0.0248(5)	1
O2	0.22476(11)	0.32620(9)	0.10386(10)	0.0268(6)	1	0.22520(12)	0.32608(10)	0.10454(11)	0.0318(6)	1
O3	0.19474(11)	0.25399(11)	0.14222(12)	0.0339(7)	1	0.19498(12)	0.25411(12)	0.14296(13)	0.0367(7)	1
O4	0.27942(11)	0.27529(12)	0.15157(9)	0.0271(6)	1	0.28025(11)	0.27474(12)	0.15191(10)	0.0307(6)	1
OW5	0.32894(11)	0.18130(11)	0.12831(11)	0.0258(6)	1	0.32873(12)	0.18079(11)	0.12810(12)	0.0330(6)	1
H5A	0.3230(30)	0.1830(30)	0.0970(9)	0.110(30)	1	0.3070(20)	0.1720(30)	0.1510(20)	0.090(20)	1
H5B	0.3080(20)	0.1720(30)	0.1510(20)	0.100(30)	1	0.3130(40)	0.1870(50)	0.1000(30)	0.190(60)	1
OW6	0.1035(4)	0.1787(4)	0.0886(4)	0.021(2)	0.2446(16)	0.1029(4)	0.1792(4)	0.0900(5)	0.027(2)	0.218(2)
OW7	0.1464(4)	0.1795(4)	0.0883(4)	0.023(2)	0.2349(16)	0.1470(4)	0.1800(5)	0.0893(4)	0.024(2)	0.205(2)
OW8	1/8	0.1980(20)	1/8	0.009(13)	0.041(3)	1/8	0.1927(8)	1/8	0.022(4)	0.154(3)

Table 2. Cont.

Atom	x	y	z	U_{eq}	s.o.f.	x	Y	Z	U_{eq}	s.o.f.
Shiv-8030										
K1	1/4	1/4	1/4	0.0321(2)	1					
Fe1	1/4	1/4	0	0.0133(1)	1					
Fe2	0.35279(1)	1/4	0.14721(1)	0.0129(1)	0.437(3)					
Mg2	0.35279(1)	1/4	0.14721(1)	0.0129(1)	0.563(3)					
Al *	1/8	1/8	1/8	0.0104(2)	1					
S1	0.23782(1)	0.27564(1)	0.11838(1)	0.01191(8)	1					
O1	0.24965(3)	0.24682(3)	0.07356(3)	0.0181(2)	1					
O2	0.22529(4)	0.32643(4)	0.10467(4)	0.0232(2)	1					
O3	0.19520(4)	0.25414(4)	0.14301(5)	0.0301(2)	1					
O4	0.28035(4)	0.27477(4)	0.15163(3)	0.0236(2)	1					
OW5	0.32866(4)	0.18092(4)	0.12827(4)	0.0256(2)	1					
H5A	0.3048(9)	0.1721(11)	0.1474(10)	0.067(9)	1					
H5B	0.3185(16)	0.1839(17)	0.0985(9)	0.123(17)	1					
OW6	0.1035(2)	0.17934(15)	0.0892(2)	0.0198(8)	0.222(1)					
OW7	0.1469(2)	0.1803(2)	0.0890(2)	0.0197(8)	0.214(1)					
OW8	1/8	0.1943(3)	1/8	0.0138 (18)	0.127(3)					

* Al position is spited into Al1, Al2 and Al3 positions, related to OW6, OW7 and OW8, respectively (by the command PART), the sum of Al1 + Al2 + Al3 is equal to 1 for each sample; atom coordinates of Al1, Al2, Al3 are the same.

Table 3. Selected bond distances for the voltaite-group minerals.

Atom1	Atom2	Bond Distance in Å				
		VK4-09	Dch-9-21-5s	Ni4225	SCCIII-14-20s	Shiv-8030
Fe1	O1	2.001(2) × 6	2.0007(14) × 6	2.008(2) × 6	2.006(2) × 6	2.002(1) × 6
	<Fe1–O>	2.001	2.008	2.006	2.006	2.002
Me2	O2	2.049(3) × 2	2.0543(16) × 2	2.055(3) × 2	2.047(3) × 2	2.039(1) × 2
Me2	O4	2.095(3) × 2	2.1056(17) × 2	2.115(3) × 2	2.088(3) × 2	2.085(1) × 2
Me2	OW5	2.061(3) × 2	2.0605(16) × 2	2.046(3) × 2	2.058(3) × 2	2.055(1) × 2
	<Me2–O>	2.068	2.073	2.072	2.064	2.060
Al ⁽¹⁾	OW6	1.876(11) × 12	1.865(6) × 12	1.860(10) × 12	1.853(11) × 12	1.864(4) × 12
Al	OW7	1.885(12) × 12	1.886(6) × 12	1.882(10) × 12	1.880(12) × 12	1.890(4) × 12
Al	OW8	1.88(3) × 6	1.92(3) × 6	1.99(7) × 6	1.84(2) × 6	1.886(9) × 6
	<Al–OW>	1.880	1.884	1.895	1.862	1.879
S1	O1	1.484(3)	1.4828(14)	1.487(3)	1.482(3)	1.484(1)
S1	O2	1.470(3)	1.4651(16)	1.471(3)	1.466(3)	1.470(1)
S1	O3	1.457(3)	1.4583(16)	1.455(3)	1.459(3)	1.460(1)
S1	O4	1.470(3)	1.4696(16)	1.467(3)	1.470(3)	1.468(1)
	<S1–O>	1.470	1.469	1.470	1.469	1.471
A ⁽²⁾ –O4		2.914(3) × 6	2.8798(15) × 6	2.882(3) × 6	2.870(3) × 6	2.8782(9) × 6
A–O3		3.288(4) × 6	3.331(2) × 6	3.301(4) × 6	3.273(4) × 6	3.2687(14) × 6
	<A–O>	3.101	3.105	3.091	3.071	3.073

⁽¹⁾ Al position is spited into Al1, Al2 and Al3 positions, related to OW6, OW7 and OW8, respectively (by the command PART), the sum of Al1 + Al2 + Al3 is equal to 1 for each sample; atom coordinates of Al1, Al2, Al3 are the same. ⁽²⁾ A = N or K.

The check-cif report notes the short contact (~2.58 Å) between the O3 atoms of SO₄ tetrahedra and the O atoms of Al(H₂O)₆ octahedra (O6w, O8w). The Al site is coordinated by O6w, O7w and O8w that are low-occupied due to disordering (Table 3). The O6w, O7w and O8w atoms are donors of hypothetical H atoms (because ideally Al is coordinated by six H₂O molecules) that have not been localized due to disorder, while the O3 atoms are acceptors of these hydrogen bonds. Taking into account the O3···O6w (or O3···O8w) distances and the geometry of H₂O molecules, we can estimate H···O3 (hydrogen-acceptor) distance as ~2.12 Å, which seems to be crystal chemically reasonable.

3.2. Chemical Composition

The morphology of voltaite-group minerals is shown in Figure 3. The empirical chemical formulae of voltaite-group minerals under study were calculated on the basis of $[(S,P,V)O_4] = 12$ per formula unit (*pfu*); the $Fe^{2+}:Fe^{3+}$ ratio was calculated by charge balance; H_2O content was calculated by stoichiometry, for 18 H_2O molecules *pfu*. The results are given in Table 4. In total, five samples are represented by four voltaite-group minerals: ammoniomagnesiovoltaite, ammoniovoltaite, voltaite and magnesiovoltaite; some of samples have near equal Mg and Fe content in the *Me2* site, according to structure refinement (Table 2), but the chemical composition (Table 4) allows unambiguous mineral identification. Noteworthy is the admixture of P and V in ammoniovoltaite from the Dachnue geothermal field and the P admixture in samples from Bolshoi Semiachik, although their contents are still too low to be detected by X-ray diffraction analysis.

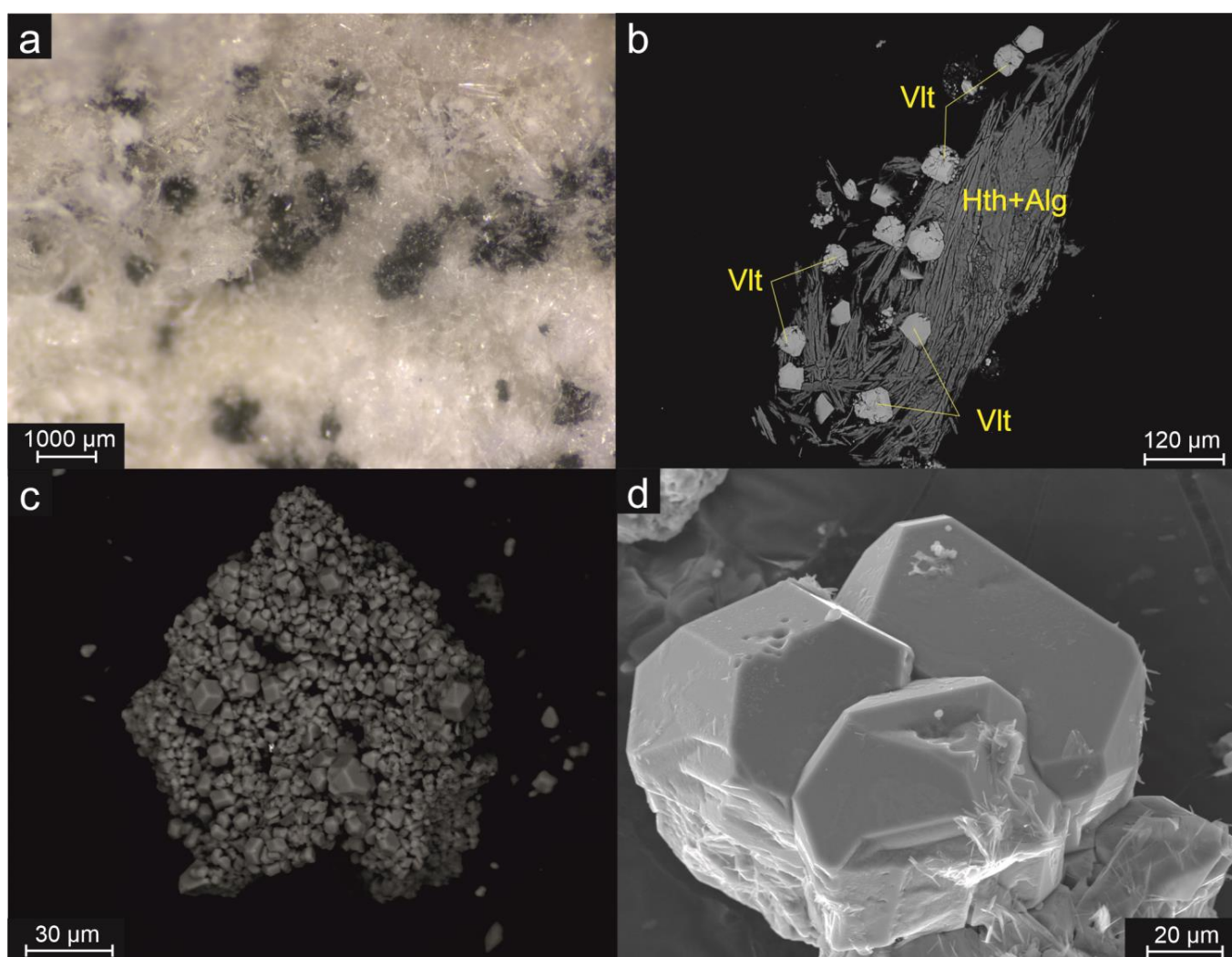


Figure 3. Voltaite-group minerals: (a) photo of black crystals of voltaite in a halotrichite-alunogen matrix, sample SCCIII-14-20s; (b) BSE image of voltaite (vlt) in association with halotrichite (hth) and alunogen (alg), sample SCCIII-14-20s; (c) BSE image of voltaite from coal fire, sample Ni4225; (d) SE image of magnesiovoltaite from Shiveluch, sample Shiv-8030.

Table 4. Chemical composition of the voltaite-group minerals studied in this work.

Sample	VK4-09	VK4-09	Dch-9-21-5s	Ni4225	SCCIII-14-20s	Shiv-8030
<i>n</i> ¹	17	10	16	9	20	5
	wt. %					
(NH ₄) ₂ O ²	2.55	2.53	2.69	0.15	0.19	n.d.
Na ₂ O	n.d.	n.d.	n.d.	0.11	0.06	n.d.
K ₂ O	0.39	0.36	n.d.	2.04	2.08	4.57
MgO	6.47	8.13	2.12	4.86	5.32	8.14
FeO	7.25	4.79	14.48	10.19	9.59	4.35
Fe ₂ O ₃	12.07	12.42	10.72	11.32	11.55	11.99
Al ₂ O ₃	3.21	3.13	3.77	3.66	3.33	3.20
TiO ₂	n.d.	n.d.	n.d.	n.d.	n.d.	0.42
SO ₃	50.89	51.60	47.23	50.60	50.33	51.39
P ₂ O ₅	n.d.	n.d.	1.57	n.d.	0.48	n.d.
V ₂ O ₅	n.d.	n.d.	0.92	n.d.	n.d.	n.d.
H ₂ O _{calc}	17.17	17.04	16.51	17.07	17.07	17.34
Total ³	100.00	100.00	100.00	100.00	100.00	101.40
	formula calculated based on [(S,P,V)O ₄] ₁₂ (H ₂ O) ₁₈					
NH ₄	1.85	1.81	2.0	0.11	0.14	-
Na	-	-	-	0.07	0.04	-
K	0.16	0.14	-	0.82	0.84	1.81
Mg	3.03	3.76	1.03	2.29	2.51	3.78
Fe ²⁺	1.90	1.24	3.96	2.69	2.54	1.13
Fe ³⁺	2.85	2.90	2.64	2.69	2.75	2.81
Al	1.19	1.14	1.45	1.36	1.24	1.18
Ti	-	-	-	-	-	0.10
S	12	12	11.59	12	11.94	12
P	-	-	0.22	-	0.06	-
V	-	-	0.20	-	-	-
H ₂ O	18	18	18	18	18	18
Mineral	Ammoniomagnesiovoltaite		Ammoniovoltaite	Voltaite		Magnesiovoltaite
(NH ₄)/K	92/8	90/10	100/0	12/88 ⁴	14/84	0/100
Fe ²⁺ /Mg	38/62	25/75	80/20	54/46	50/50	23/77
	Component's ratio according to structure refinement					
(NH ₄)/K	89/11		85/15	37/63	9/91	0/100
Fe ²⁺ /Mg	50/50		60/40	50/50	50/50	57/43
<i>a</i> , Å	27.29		27.25	27.24	27.18	27.19

n.d.—not detected. ¹ *n*—number of analyses averaged. ² A considerable amount of N is detected in EDS spectra, however, N content is determined with wide deviations. Thus, (NH₄)₂O is recalculated as sum of univalent cations equal to 2.00. ³ The total has been normalized per 100 wt. % for samples VK4-09, Dch9-21-5s, Ni4225, SKCIII-14-20s since analyses were performed from unpolished samples. ⁴ Excluding Na.

4. Discussion

In this work, four mineral species belonging to the voltaite group were studied: ammoniovoltaite, ammoniomagnesiovoltaite, voltaite and magnesiovoltaite. This quadrilateral

is due to $\text{Fe}^{2+} \leftrightarrow \text{Mg}$ and $(\text{NH}_4)^+ \leftrightarrow \text{K}$ substitutions; while trivalent cations do not show significant isomorphism. The S^{6+} (in SO_4 tetrahedra) can be substituted by small amounts of V^{5+} and P^{5+} . In the present study, ammonium members are reported from the geothermal fields together with potassium members. Potassium members are described from coal fires and solfatares at pyroclastic (volcanic) deposits, although the abundance of ammonium in these occurrences suggests that ammonium-dominant varieties can also be present there. In geothermal fields, the distribution of ammonium is local; NH_3 is carried out by steam-gas jets and then concentrated in some parts. In ammonium-depleted areas, where the acidic leaching process still takes place, potassium members may form. The study shows that ammonium members of the voltaite group are not so rare, but this is true for certain geochemical environments, such as those associated with post-volcanic processes. However, since ammonium- and potassium-dominant species are visually undistinguishable, they can be properly identified only by analytical investigation. The colour change in voltaite crystals is believed to be due to divalent cations [12]. In our collection, magnesiovoltaite is light grey to dark grey, and ammoniomagnesiovoltaite is greenish-grey, while Fe^{2+} -dominant members are black.

The crystal structures of all studied voltaite-group minerals were processed and refined in an $Fd-3c$ space group since no clear evidence of symmetry reduction was observed. All minerals are isotypic and differ only in site occupancies and corresponding bond distances. The geometrical parameters of synthetic voltaites have been described in detail by [12]. However, the crystal chemical comparison of geometrical parameters for natural voltaites is lacking. For example, before this work, for ammoniomagnesiovoltaite only powder XRD data were reported [4] and the crystal structures of some of voltaite-group representatives were obtained only as part of the new mineral description. Below we discuss some geometrical parameters relative to the chemical composition of the voltaite-group minerals.

The average S–O bond lengths of SO_4 tetrahedra are in the range 1.469–1.471 Å that agrees with the theoretical value of 1.47 Å [32] and with the range in S–O bond lengths of 1.470–1.474 Å obtained for synthetic samples [12]. Some small P and V contents were observed in the chemical composition of the voltaite-group minerals. Here we note that P admixture has been previously reported for alunite-supergroup minerals, alun-(Na) and amarillite formed at the geothermal (Dachnue) and fumarole (Donnoe) fields of the Mutnovsky volcano [33]. The P- and V-bearing ammoniovoltaite from the Dachnue geothermal field extends this trend.

In the M1O_6 octahedra the M1–O bond distances (Figure 4) vary from 2.001 to 2.008 Å, whereas theoretical Fe^{3+} –O distance calculated as the sum of ionic radii of high-spin Fe^{3+} [12] and O^{2-} is 2.005 Å [32]. As such, very minor substitution can be observed in this site.

In the $\text{Al}(\text{H}_2\text{O})_6$ polyhedra (disordered octahedral, see Figure 4), the Al–O bond lengths vary from 1.85 to 1.99 Å (Table 3) and this is likely due to strong disordering of O atoms (donors of H_2O molecules) rather than any difference in the site occupancy.

The most prominent isomorphism is observed in sites *A* and *Me2*.

The *A* site is surrounded (neglecting possible H atoms that should be surrounding N, but were impossible to localize) by six O4 atoms (at a distance 2.87–2.91 Å) and six O3 atoms (at a distance 3.27–3.33 Å). Previously, J. Majzlan and coauthors [12] noticed that ammonio voltaites have larger lattice parameters than potassium ones. The structure refinement of ammoniovoltaite [6] indirectly confirmed this since $\langle A-O \rangle$ for ammoniovoltaite was reported as 3.12 Å while potassium voltaites have $\langle A-O \rangle$ in the range 3.02–3.08 Å. The present work confirms that the incorporation of ammonium instead of potassium results in longer $\langle A-O \rangle$ distances (see values in Table 3), expanding the unit cell lattice as well (Figure 5a). The present study shows that ammonium members indeed have larger *a* unit cell parameters (27.25–27.29 Å) than potassium members (27.18–27.24 Å). For ammonio-magnesiovoltaite and ammoniovoltaite, the *a* parameter was reported as 27.26 [4] and 27.32 Å [6], respectively. The ammonium and potassium members of the voltaite group

should differ in the a unit cell parameter and can hypothetically be distinguished from each other. However, the a parameter is also determined by the size of the divalent cation, so this is still not the most reliable indicator.

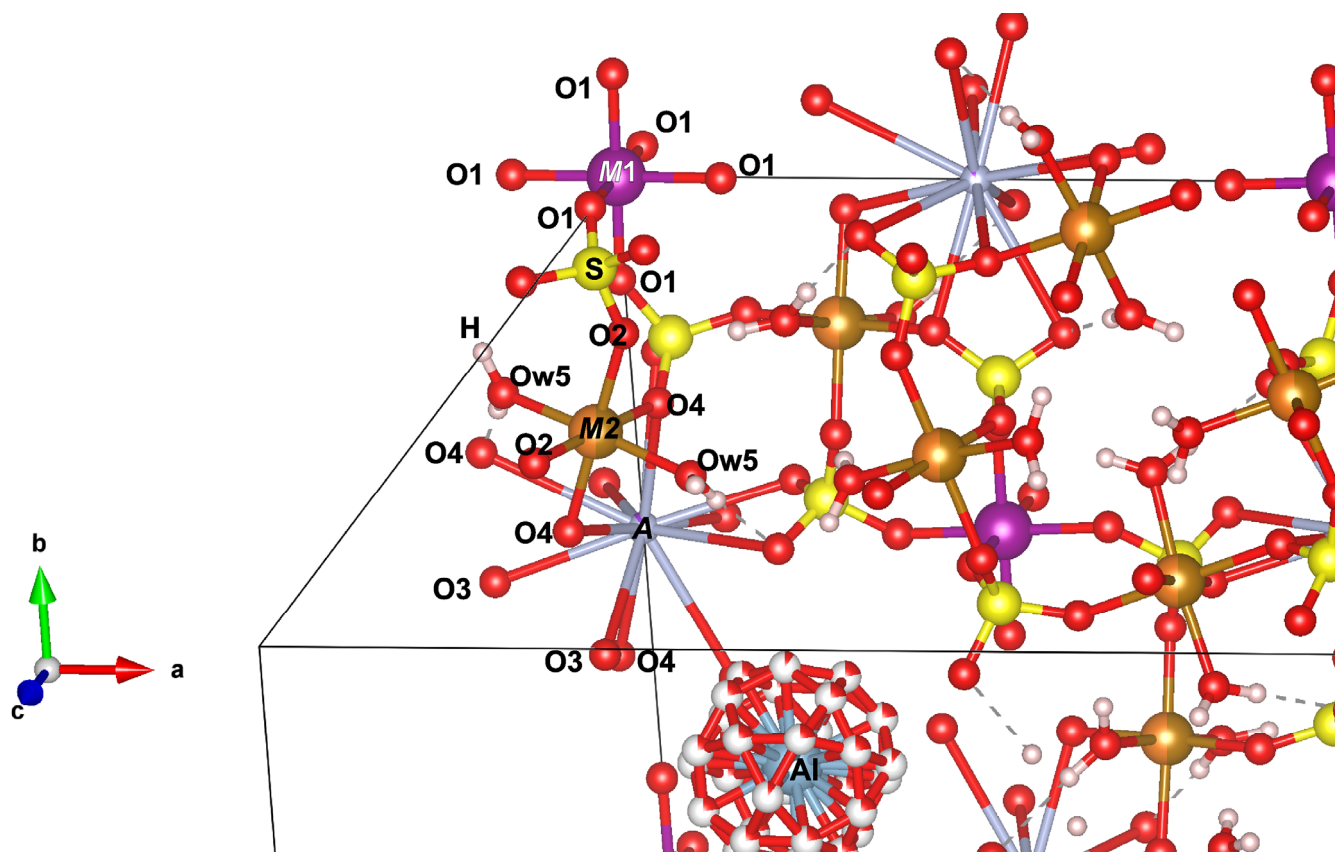


Figure 4. Part of the voltaite crystal structure showing atomic sites and some O atoms (labelled). The unit cell is outlined by black line and crystallographic axes are shown.

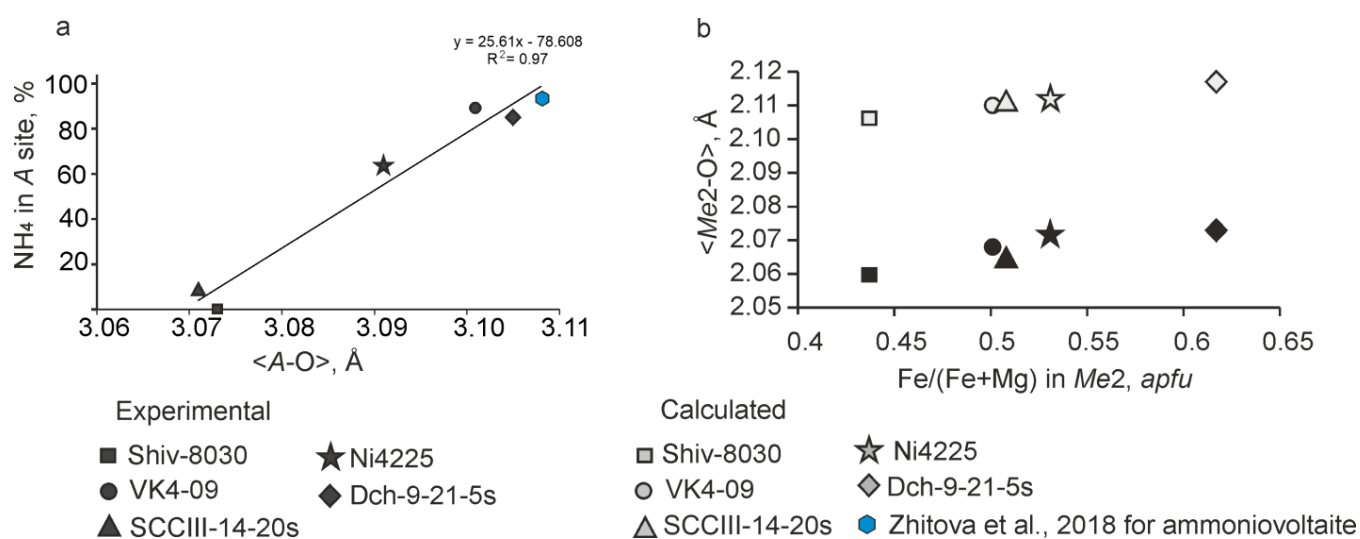


Figure 5. Correlations between (a) ammonium content and $\langle A-O \rangle$ bond distance and (b) experimental and calculated (theoretical) $M-O$ bond distances relative to Fe content Me_2 site. The data from [6] were used for the graph.

In the $Me2\phi6$ octahedra, a considerable $Me2-\phi$ bond lengths range is observed from 2.060 to 2.073 Å (Table 3), as well as Fe^{2+} -Mg isomorphic substitution. In general, longer bonds correspond to Fe^{2+} -dominant species, while shorter $Me2-\phi$ bonds are characteristic for Mg-dominant members. However, the calculation of theoretical $Me2-\phi$ bond lengths using site occupancies (or chemical composition) and ionic radii of atoms shows that experimental values are rather significantly shorter than theoretical ones; the same was observed for synthetic voltaites [12]. The $Me2-\phi$ bond lengths (2.060–2.073 Å) observed in this work (Figure 5b) agree with those reported for synthetic voltaites with $Me2\sim Fe^{2+}_{0.6}Mg_{0.4}$ [12], although the calculated value using ionic radii (of high-spin Fe^{2+} and Mg) is 2.116 Å. One possible explanation of this phenomenon could be the presence of Fe^{3+} in the $Me2$ site, however, the calculations show that the amount of Fe^{3+} should have been too considerable (as 1–1.5 *apfu*) to account for such bond length reduction, and at the same time such Fe^{3+} content is unrealistic from the position of charge compensation. For example, for sample Shiv-8030, $Me2 = Mg_{0.77}Fe_{0.23}$ (Table 3) and $\langle Me2-\phi \rangle_{obs} = 2.060$ Å, while $\langle Me2-\phi \rangle_{calc} = 2.094$ Å ($Fe = Fe^{2+}$) and 2.063 Å ($Fe = Fe^{3+}$). If we follow the variant with Fe^{3+} , then 5 *apfu* of M^{2+} turns to $\sim M^{2+}_4M^{3+}_1$ producing extra charge 1+ without any clear mechanism of charge compensation. A similar issue with $\langle Me2-\phi \rangle_{obs}$ being shorter than $\langle Me2-\phi \rangle_{calc}$ is reported for synthetic voltaites [12]: “At the nominal M^{2+} site, the bond length calculations indicate consistently high degree of mixing, with 30–50% of Fe^{3+} at this site. We note that we did not constrain these calculations with the requirement of charge sum at the two sites and therefore the results should be considered semi-quantitative”. We propose that based on the data for synthetic and natural voltaites, the mechanism of systematic shortening of $\langle Me2-\phi \rangle$ bonds cannot be explained by Fe^{3+} in the $Me2^{2+}$ site due to the requirements of chemical formula electro-neutrality. The most realistic option is that the mean $\langle Me2-\phi6 \rangle_{obs}$ bond length is shorter due to bond lengths distortion [34]. The $Me2$ site ($Me2 = Fe, Mg$) is coordinated by three symmetrically independent O atoms, O2, O4 and hydroxylated Ow5 atom (donor of two H atoms) (Figure 4), with $Me2-O2$ in the range 2.039–2.055 Å, $Me2-O4$ in the range 2.085–2.115 Å and $Me2-Ow5$ in the range 2.046–2.061 Å. The $Me2\phi6$ octahedra are indeed characterized by significant bond lengths distortion, which is estimated by Vesta [35] as from 0.008 to 0.014, where the distortion of $M1O_6$ ($M1 = Fe^{3+}$) octahedra is 0. Thus, for voltaite-type structures, the shortening of observed $Me^{2+}-\phi$ bonds relative to theoretical values based on ionic radii is possibly due to significant bond lengths distortion at that site. In this case, the correlation of observed $M^{2+}-\phi$ bonds to those previously reported for other voltaite-type structures seems to be more correct than to theoretical values. This also leads to an assumption that for voltaite-type structures, a calculation of the Fe^{2+}/Fe^{3+} ratio taking into account $M^{2+}-\phi$ bond lengths and theoretical ionic radii would not be realistic. However, such estimations based on empirical correlations built for voltaite-group minerals should give more correct values.

Author Contributions: Conceptualization, E.S.Z. and R.M.S.; methodology, E.S.Z., R.M.S., A.N.K. and A.A.Z.; software, E.S.Z., R.M.S., A.A.Z., N.S.V., E.Y.P. and V.O.Y.; formal analysis, E.S.Z., R.M.S., A.N.K., I.V.P., N.S.V., E.Y.P., V.O.Y., P.E.S. and T.F.S.; investigation, E.S.Z., R.M.S., A.N.K., A.A.Z., I.V.P., A.A.N. and V.O.D.; resources, E.S.Z., I.V.P., A.A.N. and V.O.D.; data curation, E.S.Z., A.A.Z. and I.V.P.; writing—original draft preparation, E.S.Z., R.M.S., A.N.K., A.A.Z. and I.V.P.; writing—review and editing, E.S.Z., R.M.S., A.N.K., A.A.Z., I.V.P., A.A.N., N.S.V., E.Y.P., V.O.D., V.O.Y., P.E.S. and T.F.S.; visualization, E.S.Z., A.N.K. and R.M.S.; supervision, E.S.Z., A.A.Z. and I.V.P.; project administration, E.S.Z.; funding acquisition, E.S.Z. All authors have read and agreed to the published version of the manuscript.

Funding: This research was funded by the President of the Russian Federation Grant MK-451.2022.1.5 (for the study of complex Fe sulfates). Technical support of the St. Petersburg State University Resource Centers “X-ray diffraction research methods” and “Geomodel” is carried out within the framework of SPbSU, grant No. AAAA-A19-119091190094 and No. 95439487, respectively.

Data Availability Statement: The crystallographic information files (cif) have been deposited into Cambridge Crystal Data Centre CCDC/FIZ Karlsruhe deposition under the numbers 2303615 (VK4-09), 2303616 (Dch-9-21-5s), 2303617 (Ni4225), 2303618 (SCCIII-14-20s) and 2303619 (Shiv-8030).

Acknowledgments: This research has been carried out using the facilities of the XRD and “Geo-model” Centers of the Saint Petersburg State University (SPbU). We are thankful to our colleagues Ruslan Kuznetsov, Alexey Rogozin and Ilya Bolshakov for providing photos of the samples and the geothermal fields and participation in the field work. We also thank the reviewers and editors.

Conflicts of Interest: The authors declare no conflict of interest.

References

1. Scacchi, A. Della Voltaite, nuova specie di minerale trovata nella solfatara di Pozzuoli. In *Antologia di Scienze Naturali*, 1st ed.; R. Piria: Napoli, Italy, 1841; pp. 67–71.
2. Wanmao, L.; Guoying, C.; Shurong, S. Zincovoltaita—A new sulfate mineral. *Acta Mineral. Sin.* **1987**, *4*, 307–312.
3. Ertl, A.; Dyar, M.D.; Hughes, J.M.; Brandstatter, F.; Gunter, M.E.; Prem, M.; Peterson, R.C. Pertlikite, a new tetragonal Mg-rich member of the voltaite group from Madeni Zakh, Iran. *Can. Mineral.* **2008**, *46*, 661–669. [[CrossRef](#)]
4. Szakáll, S.; Sajó, I.; Fehér, B.; Bigi, S. Ammoniomagnesiovoltaite, a new voltaite-related mineral species from Pécs-Vasas, Hungary. *Can. Mineral.* **2012**, *50*, 65–72. [[CrossRef](#)]
5. Chukanov, N.V.; Aksenov, S.M.; Rastsvetaeva, R.K.; Möhn, G.; Rusakov, V.S.; Pelov, I.V.; Scholz, R.; Eremina, T.A.; Belakovskiy, D.I.; Lorenz, J.A. Magnesiovoltaite, $K_2Mg_5Fe^{3+}_3Al(SO_4)_{12} \cdot 18H_2O$, a new mineral from the Alcaparrosa mine, Antofagasta region, Chile. *Eur. J. Mineral.* **2016**, *28*, 1005–1017. [[CrossRef](#)]
6. Zhitova, E.S.; Siidra, O.I.; Belakovskiy, D.I.; Shilovskikh, V.V.; Nuzhdaev, A.A.; Ismagilova, R.M. Ammoniovoltaite, $(NH_4)_2Fe^{2+}_5Fe^{3+}_3Al(SO_4)_{12}(H_2O)_{18}$, a new mineral from the Severo-Kambalny geothermal field, Kamchatka, Russia. *Mineral. Mag.* **2018**, *82*, 1057–1077. [[CrossRef](#)]
7. Gossner, B.; Bäuerlein, T. Hydrated sulfates containing three metals. *Ber. Dtsch. Chem. Ges.* **1930**, *63*, 2151–2155.
8. Gossner, B.; Bauerlein, T. Optical anomalies: Voltaite-like sulfates. *Neues. Jahrb. Geol. P.-A.* **1933**, *66*, 1–40.
9. Gossner, B.; Fell, E. Sulfates of the voltaite type. *Ber. Dtsch. Chem. Ges.* **1932**, *65*, 393–395.
10. Gossner, B.; Besslein, J. Hydrated sulfates of three metals. *Cent. Für Mineral. Geol. Und Paleontol.* **1934**, *1934*, 358–364.
11. Sajó, I.E. Characterization of synthetic voltaite analogues. *Eur. Chem. Bull.* **2012**, *1*, 35–36.
12. Majzlan, J.; Schlicht, H.; Wierzbicka-Wieczorek, M.; Giester, G.; Pöllmann, H.; Brömme, B.; Doyle, S.; Buth, G.; Bender Koch, C. A contribution to the crystal chemistry of the voltaite group: Solid solutions, Mössbauer and infrared spectra, and anomalous anisotropy. *Mineral. Petrol.* **2013**, *107*, 221–233. [[CrossRef](#)]
13. Košek, F.; Edwards, H.G.M.; Jehlička, J. Raman spectroscopic vibrational analysis of the complex iron sulfates clairite, metavoltine, and voltaite from the burning coal dump Anna I, Alsdorf, Germany. *J. Raman Spectrosc.* **2020**, *51*, 1454–1461. [[CrossRef](#)]
14. D’Orazio, M.; Mauro, D.; Valerio, M.; Biagioni, C. Secondary Sulfates from the Monte Arsiccio Mine (Apuan Alps, Tuscany, Italy): Trace-element budget and role in the formation of acid mine drainage. *Minerals* **2021**, *11*, 206. [[CrossRef](#)]
15. Hawthorne, F.C.; Krivovichev, S.V.; Burns, P.C. The crystal chemistry of sulfate minerals. *Rev. Mineral. Geochem.* **2000**, *40*, 1–112. [[CrossRef](#)]
16. Biagioni, C.; Mauro, D.; Pasero, M. Sulfates from the pyrite ore deposits of the Apuan Alps (Tuscany, Italy): A review. *Minerals* **2020**, *10*, 1092. [[CrossRef](#)]
17. Biagioni, C.; Mauro, D.; Pasero, M.; Bonaccorsi, E.; Lepore, G.O.; Zaccarini, F.; Skogby, H. Crystal-chemistry of sulfates from the Apuan Alps (Tuscany, Italy). VI. Tl-bearing alum-(K) and voltaite from the Fornovolasco mining complex. *Am. Mineral.* **2020**, *105*, 1088–1098. [[CrossRef](#)]
18. Mereiter, K. Die kristallstruktur des voltaits, $K_2Fe_5^{2+}Fe_3^{3+}Al[SO_4]_{12} \cdot 18H_2O$. *Tscher. Miner. Petrog.* **1972**, *18*, 185–202. [[CrossRef](#)]
19. Krivovichev, V.G.; Krivovichev, S.V.; Starova, G.L. Structural and Chemical Diversity and Complexity of Sulfur Minerals. *Minerals* **2023**, *13*, 1069. [[CrossRef](#)]
20. Zhao, F.; Gu, S. Secondary Sulfate Minerals from Thallium Mineralized Areas: Their Formation and Environmental Significance. *Minerals* **2021**, *11*, 855. [[CrossRef](#)]
21. Dunning, G.E.; Cooper, J.F. History and minerals of the Geysers Sonoma County, California. *Mineral. Rec.* **1993**, *24*, 339–354.
22. Sheveleva, R.M.; Nazarova, M.A.; Nuzhdaev, A.A.; Zhegunov, P.S.; Zhitova, E.S. Distribution and chemical composition of halotrichite from the geothermal fields of Kamchatka. Bulletin of Kamchatka Regional Association Educational-Scientific Center. *Earth. Sci.* **2023**, *2*, 5–16. [[CrossRef](#)]
23. Zhitova, E.S.; Sheveleva, R.M.; Zolotarev, A.A.; Krivovichev, S.V.; Shilovskikh, V.V.; Nuzhdaev, A.A.; Nazarova, M.A. The crystal structure of magnesian halotrichite, $(Fe,Mg)Al_2(SO_4)_4 \cdot 22H_2O$: Hydrogen bonding, geometrical parameters and structural complexity. *J. Geosci.* **2023**, *68*, 163–178. [[CrossRef](#)]
24. Zhitova, E.S.; Sheveleva, R.M.; Zolotarev, A.A.; Nuzhdaev, A.A. Atomic Arrangement, Hydrogen Bonding and Structural Complexity of Alunogen, $Al_2(SO_4)_3 \cdot 17H_2O$, from Kamchatka Geothermal Field, Russia. *Crystals* **2023**, *13*, 963. [[CrossRef](#)]
25. Kruszewski, Ł. Supergene sulphate minerals from the burning coal mining dumps in the Upper Silesian Coal Basin, South Poland. *Int. J. Coal Geol.* **2013**, *105*, 91–109. [[CrossRef](#)]
26. Balic-Žunic, T.; Garavelli, A.; Jakobsson, S.P.; Jonasson, K.; Katerinopoulos, A.; Kyriakopoulos, K.; Acquafredda, P. Fumarolic minerals: An overview of active European volcanoes. In *Updates in Volcanology, from Volcano Modelling to Volcano Geology*; Nemeth, K., Ed.; InTech: Rijeka, Croatia, 2016; pp. 267–322.25.

27. *CrysAlisPro Software System*, Version 1.171.38.46; Rigaku Oxford Diffraction: Oxford, UK, 2015.
28. Sheldrick, G.M. Crystal structure refinement with SHELXL. *Acta Crystallogr. A* **2015**, *71*, 3–8. [[CrossRef](#)] [[PubMed](#)]
29. Dolomanov, O.V.; Bourhis, L.J.; Gildea, R.J.; Howard, J.A.; Puschmann, H. OLEX2: A complete structure solution, refinement and analysis program. *J. Appl. Crystallogr.* **2009**, *42*, 339–341. [[CrossRef](#)]
30. Jeffrey, G.A. *An Introduction to Hydrogen Bonding*; Oxford University Press: New York, NY, USA, 1977.
31. Wilson, A.J.C. Refinement of R_2 and R_1 : A physical interpretation. *Acta Crystallogr. A* **1976**, *32*, 781–783. [[CrossRef](#)]
32. Shannon, R.D. Revised effective ionic radii and systematic studies of interatomic distances in halides and chalcogenides. *Acta Crystall. A Cryst.* **1976**, *32*, 751–767. [[CrossRef](#)]
33. Zhitova, E.S.; Khanin, D.A.; Nuzhdaev, A.A.; Nazarova, M.A.; Ismagilova, R.M.; Shilovskikh, V.V.; Kupchinenko, A.N.; Kuznetsov, R.A.; Zhegunov, P.S. Efflorescent sulphates with M^+ and M^{2+} cations from fumarole and active geothermal fields of Mutnovsky Volcano (Kamchatka, Russia). *Minerals* **2022**, *12*, 600. [[CrossRef](#)]
34. Gagné, O.C.; Hawthorne, F.C. Bond-length distributions for ions bonded to oxygen: Alkali and alkaline-earth metals. *Acta Crystallogr. B* **2016**, *72*, 602–625. [[CrossRef](#)]
35. Momma, K.; Izumi, F. VESTA: A three-dimensional visualization system for electronic and structural analysis. *J. Appl. Crystallogr.* **2008**, *41*, 653–658. [[CrossRef](#)]

Disclaimer/Publisher’s Note: The statements, opinions and data contained in all publications are solely those of the individual author(s) and contributor(s) and not of MDPI and/or the editor(s). MDPI and/or the editor(s) disclaim responsibility for any injury to people or property resulting from any ideas, methods, instructions or products referred to in the content.